

# Computational Study on the Nature of Bonding between Silver Ions and Nitrogen Ligands

Lam H. Nguyen, Dung P. Tran, and Thanh N. Truong\*

Cite This: *ACS Omega* 2022, 7, 45231–45238

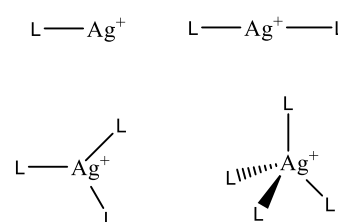
Read Online

ACCESS |

Metrics &amp; More

Article Recommendations

**ABSTRACT:** In this paper, the nature of silver ion–nitrogen atom bonding in the complexation with ammonia, azomethine, pyridine, and hydrogen cyanide from one to four coordinations is studied at the B97-1 level of density functional theory. The results indicate that the two-coordinated complex of the silver ion with different nitrogen ligands representing  $sp$ ,  $sp^2$ , and  $sp^3$  orbital hybridizations is the most stable form having the shortest  $Ag^+–N$  bond distance, highest vibrational frequencies, largest bond order, and favorable Gibbs free energy of formation. Natural bond orbital analyses further show that  $\sigma$ -donation from the nitrogen lone pair to the silver empty  $5s$  orbital is dominant in the dative metal–ligand bonding character with  $N–sp^3$  having the largest contribution among the different N atomic orbital hybridizations. Natural energy decomposition analyses further show that the two-coordinated complexes have enhanced electrostatic interaction and charge transfer energies over other coordination types leading them to be more stable. For this reason, the two-coordinated complexes would be a better representation for studying bonding and interaction in silver ion complexes.

The nature of  $Ag^+–N$  bonding in silver ion complex

Ligand (L): ammonia, azomethine, pyridine, and hydrogen cyanide

## 1. INTRODUCTION

A silver ion ( $Ag^+$ ) with its electron configuration  $[Kr] 4d^{10}5s^0$  can form stable complexes with up to six ligands from its empty  $5s$  valence orbital.<sup>1</sup> The two-coordinated form is the most common and is often used for fabricating 1D metal–organic nanostructures.<sup>2</sup> Silver ions in this coordination can link pyridyl–ferrocene ligands together through a doubly bridged connection to form a nanotube structure, as reported by Aida et al.<sup>2</sup> Three- and four-coordinated complexes are less common and often formed from sulfur- and phosphorous-based ligands for luminescent materials.<sup>3,4</sup> Five- and six-coordinated complexes are rare since their Gibbs free energies of formation are unfavorable.<sup>5</sup>

There have been a number of theoretical studies on the nature of metal–ligand chemical bonding of silver ion complexes. These studies examined metal ion–ligand interaction by either changing the type of metal ion while keeping the ligand the same or changing the type of ligand while keeping the metal ion the same. For example, a study of platinum, magnesium, copper, and gold ions with pyridine ligands,<sup>6</sup> differences in the complexation of  $Mg^{2+}$  and  $Ag^+$  ions with ammonia ( $NH_3$ ) ligands,<sup>5</sup> or a comparison study of  $Cu^+$  and  $Ag^+$  complexing with pyridine in the gas phase.<sup>7</sup> These studies show that  $Ag^+$  has smaller binding energy compared to  $Cu^+$  and  $Au^+$  ions when forming a one-coordinated complex with ammonia and pyridine ligands, and the electrostatic interaction is dominant as expected. Second, changing different types of ligands from electron-withdrawing to -donating groups

enables studies of the effects of the ligand field on the electronic and thermodynamic properties of the complexes. For example, electron-donating groups such as methyl ( $-X$ ) in organonitriles ( $NC-X$ ) strengthen the  $Ag–N$  bond.<sup>8</sup> Also, Luna et al.<sup>9</sup> have shown that  $N–sp^3$  in methyl amine has the largest charge donation in the complexation with the  $Cu^+$  ion, whereas the HCN ligand is the poorest.

Experimental studies, on the other hand, have been limited to those complexes that are stable under experimental conditions. For example, thermodynamic properties such as entropy, enthalpy, and Gibbs free energy changes for a  $Ag^+$  ion complexing with one to four ammonia ligands were able to be measured.<sup>10</sup> Experimentally, a common representative of the  $sp^2$ –nitrogen ligand is pyridine.<sup>11,12</sup> For instance, one- and two-coordinated silver–pyridine complexes were studied in solution,<sup>13</sup> while three- and four-coordinated silver–pyridine complexes were studied in the gas phase.<sup>10</sup> However, when comparing the differences in the effects of nitrogen atomic orbital hybridization on  $Ag^+$  ion–ligand bonding, the  $sp^2$  nitrogen in azomethine ( $NH=CH_2$ ) would be more suitable

Received: September 3, 2022  
Accepted: October 20, 2022  
Published: November 28, 2022



Table 1. List of All  $[\text{AgL}_n]^+$  Complexes Considered in This Study<sup>a</sup>

Number of Ligand	$\text{NH}_3$ (ammonia)		$\text{C}_5\text{H}_5\text{N}$ (pyridine)		$\text{CH}_3\text{N}$ (azomethine)		$\text{HCN}$ (hydrogencyanide)	
n = 1	N1		Py1		AM1		CN1	
n = 2	N2		Py2		AM2		CN2	
n = 3	N3		Py3		AM3		CN3	
n = 4	N4		Py4		AM4		CN4	

<sup>a</sup>Light-blue balls represent silver atoms (Ag), dark-blue for nitrogen atoms (N), gray for carbon (C), and white for hydrogen (H) atoms. Relative orientations of ligands in these complexes are also shown.

since it is not complicated by the aromaticity effects as that in pyridine. Unfortunately, there is no experimental data for the silver ion complex with azomethine. In addition, only a two-coordinated complex of a silver ion with hydrogen cyanide ligands was successfully synthesized.<sup>14</sup>

Previous theoretical studies found that electrostatic energy dominates in  $\text{Ag}^+$ –ligand interaction as expected for ion–dipole intermolecular interaction. Interestingly, the bonding from the ligand back donation was also found to enhance the ion–ligand binding energy and to affect geometries of the complexes.<sup>15,16</sup> However, such a conclusion was drawn from results of one-coordinated silver ion complexes with different types of ligands. It is known that the two-coordinated complexes are often more stable in nature as compared to one-coordinated complexes. Thus, question is whether such a finding on the role of the bonding is generally valid in all coordination cases. Furthermore, the bonding in silver ion complexes is known to have a dative bond nature with contribution from both  $\sigma$  donation and  $\pi$ -back donation.<sup>17</sup> To the best of our knowledge, there has not been any study on the effects of nitrogen atomic orbital hybridizations on the nature of this  $\text{Ag}^+$ –N dative bond.

In this study, a systematic computational study with the aim to understand the nature of chemical bonding in a silver ion complexing with ligands that have different hybridizations was carried out. In particular, three different nitrogen-based ligands, namely, ammonia ( $\text{NH}_3$ ), azomethine ( $\text{NH}=\text{CH}_2$ ), pyridine ( $\text{C}_5\text{H}_5\text{N}$ ), and hydrogen cyanide (HCN), correspond to  $\text{sp}^3$ ,  $\text{sp}^2$ , and  $\text{sp}$  hybridizations, respectively. These ligands can form one- to four-coordinated complexes with the silver ion. This allows the examination of the effects of the coordination number on the geometry, energetics, thermodynamics, and metal ion–ligand bonding characteristics of the complexes in detail and systematically.

## 2. COMPUTATIONAL DETAILS

In this study, all complexes between  $\text{Ag}^+$  and ammonia, azomethine, pyridine, and hydrogen cyanide are fully optimized in the gas phase using the Gaussian16 package<sup>18</sup> at the B97-1 level of density functional theory (DFT). B97-1<sup>19</sup> has been known to provide accurate geometries and electronic properties of transition metal complexes.<sup>20,21</sup> Also, this basis set was found to be among the most accurate DFT functionals for studying transition metal chemistry by Truhlar and Cramer,<sup>22</sup> for example, the bond energy, geometries, and dipole moment of palladium complexes.<sup>23</sup> A composite basis is used, in particular, cc-pVTZ-pp for the Ag atom and cc-pVTZ for other atoms.<sup>24</sup> The basis set superposition error is also calculated by the counterpoise method.<sup>25</sup> Table 1 summarizes the list of all complexes considered in this study and also shows their 3D configurations.

For thermodynamic analysis, enthalpy change ( $\Delta H$ ), entropy change ( $\Delta S$ ), and Gibbs free energy change ( $\Delta G$ ) of these complexes are calculated from products of translational, rotational, vibrational, and electronic partition functions using the standard statistical mechanics method. For the vibrational partition function, harmonic approximation is used. For hindered internal rotation vibrational modes of ligands around the ion–ligand bond, correction terms to the vibrational partition functions based on Truhlar's approximation are included.<sup>26</sup>

Natural population and natural energy decomposition analyses (NEDA)<sup>27</sup> were done using the natural bond orbital 7 program<sup>28</sup> attached on Gaussian16. Note that the extended transition state combined with the natural orbital for chemical valence theory (ETS-NOCV)<sup>29</sup> is another well-known methodology for energy decomposition analyses. A recent comparison study by Li and Lu<sup>30</sup> on energy component analyses for metal complexes has shown that both ETS-NOCV and NEDA yield similar results. Metal ion–ligand binding energies are decomposed into five different potential energy

**Table 2.** Calculated and Available Experimental Data for Average Ag<sup>+</sup>–N Bond Distances (Å) and Its Stretching Frequencies (cm<sup>-1</sup>) of Silver Ion Complexes with Ammonia, Azomethine, Pyridine, and Hydrogen Cyanide

complexes		$D_{\text{Ag-N}} (\text{Å})$		$\nu(\text{Ag-N}) \text{ cm}^{-1}$			
				experiment		this study	
		experiment	this study	$\nu_a$	$\nu_s$	$\nu_a$	$\nu_s$
[Ag(NH <sub>3</sub> ) <sub>n</sub> ] <sup>+</sup>	N1		2.196			372	
	N2	2.110–2.165 <sup>a</sup>	2.145	430–476 <sup>a</sup>	369–400 <sup>a</sup>	423	348
	N3	2.265 <sup>b</sup>	2.317			261	274
	N4		2.412			254	226
[Ag(AM) <sub>n</sub> ] <sup>+</sup>	AM1		2.160			368	
	AM2		2.104			410	215
	AM3		2.258			311	160
	AM4		2.356			273	256
[Ag(Py) <sub>n</sub> ] <sup>+</sup>	Py1		2.155			203	
	Py2	2.128–2.180 <sup>c</sup>	2.115	226–230 <sup>c</sup>	157–166 <sup>c</sup>	252	156
	Py3	2.245; 2.587 <sup>d</sup>	2.181, 2.585	190 <sup>d</sup>	145 <sup>d</sup>	228	142
	Py4	2.322 <sup>e</sup>	2.384	122 <sup>e</sup>	88 <sup>e</sup>	122	117
[Ag(NCH) <sub>n</sub> ] <sup>+</sup>	CN1		2.148			273	
	CN2	2.130 <sup>f</sup>	2.080			348	267
	CN3		2.222			242	224
	CN4		2.323			172	171

<sup>a</sup>[Ag(NH<sub>3</sub>)<sub>2</sub>]<sub>2</sub>SO<sub>4</sub>;<sup>35,36</sup> [Ag(NH<sub>3</sub>)<sub>2</sub>]ClO<sub>4</sub>;<sup>37,38</sup> [Ag(NH<sub>3</sub>)<sub>2</sub>]NO<sub>3</sub>;<sup>36,37</sup> <sup>b</sup>[Ag(NH<sub>3</sub>)<sub>3</sub>]ClO<sub>4</sub>;<sup>37</sup> <sup>c</sup>[Ag(Py)<sub>2</sub>]ClO<sub>4</sub>;<sup>39</sup> [Ag(Py)<sub>2</sub>]NO<sub>3</sub>;<sup>11</sup> <sup>d</sup>[Ag(Py)<sub>3</sub>]-NO<sub>3</sub>;<sup>34</sup> <sup>e</sup>[Ag(Py)<sub>4</sub>]ClO<sub>4</sub>;<sup>39</sup> <sup>f</sup>[Ag(HCN)<sub>2</sub>]SbF<sub>6</sub>.<sup>14</sup>

terms, namely, electrostatic—ES, polarization—POL, exchange correlation—XC, charge transfer—CT, and deformation—DEF, by NEDA.<sup>27,31–33</sup>

### 3. RESULTS AND DISCUSSION

**3.1. Geometries and Vibrational Spectra.** As shown in Table 1, the optimized silver complexes with two ligands have a linear configuration; namely, the angles N–Ag<sup>+</sup>–N are close to 180°. Furthermore, two ammonias are in the eclipsed configuration, whereas the two azomethines are perpendicular to each other. For the two-coordinated complex with pyridine, there are two nearly degenerate local stable structures, namely, in-plane where the two pyridine rings are in the same plane and out-of-plane where the two pyridines are perpendicular to each other, with a difference in energy of less than 1.0 kcal/mol. In this study, further calculations and analyses were done for the in-plane conformation due to its correspondence with the experimental crystal structure.<sup>34</sup>

Three-coordinated complexes with ammonia, azomethine, and hydrogen cyanide ligands have trigonal shapes, whereas the complex with pyridine is close to a T-shape with two N–Ag<sup>+</sup>–N angles having values of 160 and 99.5°. Four-coordinated complexes all have the tetrahedral configuration with the N–Ag<sup>+</sup>–N angle around 109°.

Table 2 lists the optimized Ag<sup>+</sup>–N bond distances in all complexes and their corresponding vibrational frequencies along with available experimental data. Note that some experiments were done in solution, and thus, its data include effects of counter ions and solvent–solute interactions, whereas calculated results presented here are for isolated complexes.

First, as shown in Figure 1 and Table 2, the calculated complex bond distances are close to those from the experimental data for each hybridization type and generally increase with the larger coordination number with the exception of the two-coordinated configuration, which has the shortest bond distance. These results suggest that the two-

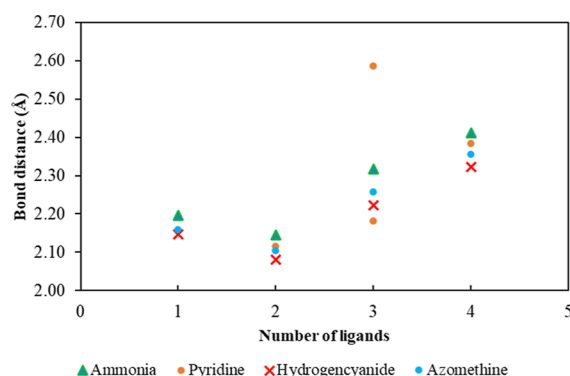


**Figure 1.** Plot of Ag<sup>+</sup>–N bond distances vs the coordination number for four ligand types: ammonia (green triangle), azomethine (blue dot), pyridine (orange dot), and hydrogen cyanide (red cross).

coordinated complexes may have significantly other bonding characters such as the bonding that is beyond strictly intermolecular interaction. For the three-coordinated complex with pyridine, it has a T-shape configuration with the shorter bond distance for the two nearly linear ligands and the longer bond distance for the other. This configuration suggests the preference for T-shape interaction between a pair of pyridines similar to that of a benzene dimer. For each coordination number, the Ag<sup>+</sup>–N bond distance is generally the shortest for the N–sp hybridization and the longest for sp<sup>3</sup> hybridization.

Second, an excellent agreement between computed and experimental frequencies for the Ag<sup>+</sup>–N vibrational modes is observed. In particular, the asymmetric stretch ( $\nu_a$ ) signals at 423 cm<sup>-1</sup> in [Ag(NH<sub>3</sub>)<sub>2</sub>]<sup>+</sup> and 252 cm<sup>-1</sup> in [Ag(Py)<sub>2</sub>]<sup>+</sup> are not much different from the experimental values of 430 and 226 cm<sup>-1</sup>, respectively.<sup>34,35</sup> Also, the calculated symmetric vibrations ( $\nu_s$ ) of different complexes are within the range of various experimental data.

It is known that as the bond energy increases, its bond distance decreases, and its stretching vibrational frequency

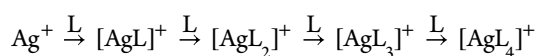
**Table 3. Standard Enthalpy Changes (kcal mol<sup>-1</sup>), Entropy Changes (cal mol<sup>-1</sup> K<sup>-1</sup>), and Gibbs Free Energy Changes (kcal mol<sup>-1</sup>) of the Stepwise Reaction [Ag(L)<sub>n</sub>]<sup>+</sup> + L → [Ag(L)<sub>n+1</sub>]<sup>+</sup> (n = 0–3) at 298 K<sup>a</sup>**

[Ag(L) <sub>n</sub> ] <sup>+</sup> + L → [Ag(L) <sub>n+1</sub> ] <sup>+</sup>	ΔS <sub>R</sub> <sup>0</sup>	ΔH <sub>R</sub> <sup>0</sup>	ΔG <sub>R</sub> <sup>0</sup>	relative ΔH <sub>R</sub> <sup>0</sup>	relative ΔG <sub>R</sub> <sup>0</sup>
Ag <sup>+</sup> + NH <sub>3</sub> → [Ag(NH <sub>3</sub> )] <sup>+</sup>	-22.4	-46.18	-39.49	4.77	4.08
[Ag(NH <sub>3</sub> )] <sup>+</sup> + NH <sub>3</sub> → [Ag(NH <sub>3</sub> ) <sub>2</sub> ] <sup>+</sup>	-35.8	-43.65 (-36.90 <sup>b</sup> )	-32.97 (-27.20 <sup>b</sup> )	4.51 (2.84)	3.41 (6.63)
[Ag(NH <sub>3</sub> ) <sub>2</sub> ] <sup>+</sup> + NH <sub>3</sub> → [Ag(NH <sub>3</sub> ) <sub>3</sub> ] <sup>+</sup>	-13.5	-11.92 (-14.60 <sup>b</sup> )	-11.92 (-7.300 <sup>b</sup> )	1.23 (1.12)	1.23 (1.78)
[Ag(NH <sub>3</sub> ) <sub>3</sub> ] <sup>+</sup> + NH <sub>3</sub> → [Ag(NH <sub>3</sub> ) <sub>4</sub> ] <sup>+</sup>	-27.1	-9.68 (-13.00 <sup>b</sup> )	-9.68 (-4.100 <sup>b</sup> )	1.00 (1.00)	1.00 (1.00)
Ag <sup>+</sup> + NHCH <sub>2</sub> → [Ag(NHCH <sub>2</sub> )] <sup>+</sup>	-25.1	-47.36	-39.87	4.83	29.32
[Ag(NHCH <sub>2</sub> )] <sup>+</sup> + NHCH <sub>2</sub> → [Ag(NHCH <sub>2</sub> ) <sub>2</sub> ] <sup>+</sup>	-32.6	-44.02	-34.32	4.49	25.54
[Ag(NHCH <sub>2</sub> ) <sub>2</sub> ] <sup>+</sup> + NHCH <sub>2</sub> → [Ag(NHCH <sub>2</sub> ) <sub>3</sub> ] <sup>+</sup>	-19.7	-11.21	-5.340	1.14	3.92
[Ag(NHCH <sub>2</sub> ) <sub>3</sub> ] <sup>+</sup> + NHCH <sub>2</sub> → [Ag(NHCH <sub>2</sub> ) <sub>4</sub> ] <sup>+</sup>	-28.3	-9.80	-1.360	1.00	1.00
Ag <sup>+</sup> + NC <sub>3</sub> H <sub>5</sub> → [Ag(NC <sub>3</sub> H <sub>5</sub> )] <sup>+</sup>	-25.7	-52.66 (-48.60 <sup>c</sup> )	-45.01	5.46 (2.94)	20.56
[Ag(NC <sub>3</sub> H <sub>5</sub> )] <sup>+</sup> + NC <sub>3</sub> H <sub>5</sub> → [Ag(NC <sub>3</sub> H <sub>5</sub> ) <sub>2</sub> ] <sup>+</sup>	-42.7	-46.19	-33.46	4.79	15.28
[Ag(NC <sub>3</sub> H <sub>5</sub> ) <sub>2</sub> ] <sup>+</sup> + NC <sub>3</sub> H <sub>5</sub> → [Ag(NC <sub>3</sub> H <sub>5</sub> ) <sub>3</sub> ] <sup>+</sup>	-28.3	-10.63 (-16.70 <sup>d</sup> )	-2.189 (-8.400 <sup>d</sup> )	1.10 (1.00)	1.00 (1.42)
[Ag(NC <sub>3</sub> H <sub>5</sub> ) <sub>3</sub> ] <sup>+</sup> + NC <sub>3</sub> H <sub>5</sub> → [Ag(NC <sub>3</sub> H <sub>5</sub> ) <sub>4</sub> ] <sup>+</sup>	-24.3	-9.64 (-17.90 <sup>d</sup> )	-2.398 (-5.900 <sup>d</sup> )	1.00 (1.07)	1.10 (1.00)
Ag <sup>+</sup> + HCN → [Ag(HCN)] <sup>+</sup>	-15.5	-36.66 (-40.10 <sup>e</sup> )	-32.04 (-33.30 <sup>e</sup> )	3.94 (3.71)	5.99 (9.79)
[Ag(HCN)] <sup>+</sup> + HCN → [Ag(HCN) <sub>2</sub> ] <sup>+</sup>	-24.7	-36.17 (-35.30 <sup>e</sup> )	-28.80 (-27.40 <sup>e</sup> )	3.89 (3.27)	5.38 (8.06)
[Ag(HCN) <sub>2</sub> ] <sup>+</sup> + HCN → [Ag(HCN) <sub>3</sub> ] <sup>+</sup>	-8.80	-12.03 (-15.90 <sup>e</sup> )	-9.400 (-9.100 <sup>e</sup> )	1.29 (1.47)	1.76 (2.68)
[Ag(HCN) <sub>3</sub> ] <sup>+</sup> + HCN → [Ag(HCN) <sub>4</sub> ] <sup>+</sup>	-13.3	-9.300 (-10.80 <sup>e</sup> )	-5.350 (-3.400 <sup>e</sup> )	1.00 (1.00)	1.00 (1.00)

<sup>a</sup>Values in the parentheses are from the experiment or previous calculations. <sup>b</sup>Experimental data taken from ref 5. <sup>c</sup>Experimental data taken from ref 13. <sup>d</sup>Experimental data taken from ref 10. <sup>e</sup>Computed data at the B3LYP/DZVP level of theory taken from ref 8.

shifts toward a larger wavenumber. Such a trend is observed here for a Ag ion complexing with different ligands in different coordination configurations. In particular, the two-coordinated complexes with the shortest Ag<sup>+</sup>–N bond distances as compared to those of other coordinated forms have the largest frequencies for their asymmetric stretching vibrations. In fact, a similar trend in the bond distance versus the coordination number as shown in Figure 1 is also observed for the asymmetric stretching frequencies but in the opposite direction.

**3.2. Thermodynamic Analysis.** It is common to study the thermochemistry of the complex formation reaction as functions of the coordination number by using the step-wise mechanism as follows



All computed values of standard enthalpy change, entropy change, and Gibbs free energy change at the room temperature (298 K) along with results from previous experimental or computed data are presented in Table 3. Specifically, for silver–hydrogen cyanide complexes, previous theoretical data up to six coordinations are available<sup>8</sup> but not experimentally. On the other hand, for silver–ammonia with up to four ligands and for silver–pyridine complexes with one, three, and four ligands,<sup>10</sup> experimental data in the gas phase are available for comparison. For comparison with previous data, relative changes for each type of ligand for both enthalpy and Gibbs free energies, ΔH<sub>R</sub><sup>0</sup> and ΔG<sub>R</sub><sup>0</sup>, by dividing by their smallest values are also reported.

First, entropies of formation of the two-coordinated complexes for all ligand types are the largest (most negative) as compared to those of other corresponding coordinated forms. This is consistent with the trends observed in Ag<sup>+</sup>–N bond distances and vibrational frequencies of these complexes. Second, within each ligand type, enthalpies of formation for the one- and two-coordinated complexes are about 4 times larger than those of three- and four-coordinated complexes.

Combined with the entropies of formation, the Gibbs free energies of step-wise complex formation for the one- and two-coordinated complexes within each ligand type are significantly larger than those of three- and four-coordinated forms. These suggest that one- and two-coordinated complexes are more prevalent at the room temperature for all ligand types. This is consistent with the experiment finding that one- and two-coordinated forms of pyridine complexes compete with each other.<sup>40,41</sup>

Excellent agreement with the available experimental data presented above indicates that the wavefunction at the level of theory used in this study is reasonably accurate for further analyses of the bonding nature of the Ag ion with various ligands as presented below.

**3.3. NBO Analyses.** Table 4 summarizes results from the natural population analyses for all complexes. First, notice the strong drop in the Ag ion charge in the two-coordinated complexes as compared to that in other coordination forms for all ligands. This again demonstrates special bonding characters for the two-coordinated complexes. The changes in the silver ion charge per ligand also indicate that only one- and two-coordinated forms have significant changes in the interaction nature of the silver ion with different types of ligands. Higher-coordinated forms have small effects on this nature.

Wiberg bond index (WBI) analyses also indicate that the bond orders for the Ag<sup>+</sup>–N bonds in the one- and two-coordinated complexes are noticeably larger than those of higher order-coordinated complexes for each type of ligand. More specifically, for each ligand type, the two-coordinated complex has the highest bond order (nearly 0.3) in all cases. It is interesting to note that for the three-coordinated complex with pyridine, the two nearly linear Ag<sup>+</sup>–N bonds have WBI values of 0.22 which is close to the value of 0.27 of the two-coordinated complex, while the WBI of the third (middle) pyridine ligand is nearly 0 indicating strictly electrostatic interaction. Natural resonance theory analyses further support these results showing that the majority of the Ag<sup>+</sup>–N bonding characters in all complexes are ionic with contribution of more than 80%. Again, consistent with other calculated results, the one- and two-coordinated complexes have noticeable bonding

**Table 4. Silver Atomic Charge  $Q_{Ag}$  from NBO Analyses, Charge Change per Ligand  $\Delta Q_{Ag} = \frac{1-Q_{Ag}}{n}$ , WBI, and Percentages of Covalent and Ionic Characters in the Silver–Nitrogen Bond Calculated Based on Natural Resonance Theory**

complexes	$Q_{Ag}$	$\Delta Q_{Ag}$	WBI	NRT		
				ionic (%)	covalent (%)	
[Ag(NH <sub>3</sub> ) <sub>n</sub> ] <sup>+</sup>	N1	0.89	0.12	0.26	87	13
	N2	0.68	0.16	0.29	81	19
	N3	0.74	0.08	0.18	90	10
	N4	0.75	0.06	0.13	91	9
[Ag(NHCH <sub>2</sub> ) <sub>n</sub> ] <sup>+</sup>	AM1	0.89	0.11	0.24	88	12
	AM2	0.71	0.15	0.28	82	18
	AM3	0.80	0.07	0.17	91	9
	AM4	0.81	0.05	0.12	96	4
[Ag(NC <sub>5</sub> H <sub>5</sub> ) <sub>n</sub> ] <sup>+</sup>	Py1	0.86	0.14	0.26	86	14
	Py2	0.70	0.15	0.27	83	17
	Py3	0.75	0.08	0.22	88	12
	Py4	0.82	0.04	0.10	0	0
[Ag(NCH) <sub>n</sub> ] <sup>+</sup>	CN1	0.96	0.04	0.15	94	6
	CN2	0.82	0.09	0.24	88	12
	CN3	0.89	0.04	0.15	94	6
	CN4	0.89	0.03	0.11	96	4

characters with the largest contribution of covalent character found in the two-coordinated form as compared to other coordinated forms for each ligand type.

Natural bond orbital (NBO) analyses can provide further information on the dative bond between the silver ion and the ligands. In particular, second-order perturbation theory<sup>42</sup> can be used to calculate energy release upon  $\sigma$ -donation and  $\pi$ -back donation in the dative bond component of the metal–ligand interaction.

In general, for all complexes studied here, the  $\sigma$ -donation is from the nitrogen lone pairs to the empty silver 5s orbital, whereas the  $\pi$ -back donation is from the silver (4d)<sup>10</sup> to the virtual  $\pi^*$  orbitals of the ligands.

Table 5 lists all donor–acceptor orbital charge transfer energies from NBO analyses which are above 1.0 kcal/mol. Note that in all cases,  $\sigma$ -donations from nitrogen lone pairs to the silver 5s<sup>0</sup> orbital are significantly larger by many orders of magnitude compared to those of the  $\pi$ -back donation where existing. Furthermore, within each ligand type, the magnitude of donor–acceptor orbital energy release for the two-coordinated complexes is noticeably larger than that of other coordinated forms. These results suggest that additional stabilization observed in the two-coordinated complexes is due mainly to the  $\sigma$ -donation bonding component. A similar phenomenon was presented in a comparison of the bond strength of Ag<sup>+</sup>–O and Ag<sup>+</sup>–N in Ma's study.<sup>15</sup> Upon comparing the orbital charge transfer energies released in all two-coordinated complexes, it is seen that the nitrogen lone pair from the sp<sup>3</sup> orbital has the largest  $\sigma$ -donation value, while the sp orbital has the smallest. This may be due to the fact that the nitrogen sp<sup>3</sup> orbital has larger p character than sp<sup>2</sup> and sp orbitals and thus would have larger overlap with the silver 5s orbital. Furthermore,  $\sigma$ -donation energy transfers of the complexes with pyridines are larger compared to those of silver–azomethine complexes. This indicates that electrons

**Table 5. Average Donor–Acceptor Interaction Energy (kcal/mol) in the Complex of the Silver Ion with Ligands: Ammonia, Azomethine, Pyridine, and Hydrogen Cyanide<sup>a</sup>**

complex	donor	acceptor	$E_{ave}$	
[Ag(NH <sub>3</sub> ) <sub>n</sub> ] <sup>+</sup>	N1	N: sp <sup>3</sup> lone pair	Ag <sup>+</sup> : 5s <sup>0</sup>	43.32 (1)
	N2	N: sp <sup>3</sup> lone pair	Ag <sup>+</sup> : 5s <sup>0</sup>	81.05 (2)
	N3	N: sp <sup>3</sup> lone pair	Ag <sup>+</sup> : 5s <sup>0</sup>	56.80 (3)
	N4	N: sp <sup>3</sup> lone pair	Ag <sup>+</sup> : 5s <sup>0</sup>	54.97 (4)
[Ag(NHCH <sub>2</sub> ) <sub>n</sub> ] <sup>+</sup>	AM1	N: sp <sup>2</sup> lone pair	Ag <sup>+</sup> : 5s <sup>0</sup>	36.28 (1)
		Ag <sup>+</sup> : 4d <sup>10</sup>	$\pi_{C=N}^*$	1.930 (2)
	AM2	N: sp <sup>2</sup> lone pair	Ag <sup>+</sup> : 5s <sup>0</sup>	68.84 (2)
		Ag <sup>+</sup> : 4d <sup>10</sup>	$\pi_{C=N}^*$	1.390 (4)
	AM3	N: sp <sup>2</sup> lone pair	Ag <sup>+</sup> : 5s <sup>0</sup>	44.62 (3)
		Ag <sup>+</sup> : 4d <sup>10</sup>	$\pi_{C=N}^*$	1.230 (3)
	AM4	N: sp <sup>2</sup> lone pair	Ag <sup>+</sup> : 5s <sup>0</sup>	40.44 (4)
[Ag(NC <sub>5</sub> H <sub>5</sub> ) <sub>n</sub> ] <sup>+</sup>	Py1	N: sp <sup>2</sup> lone pair	Ag <sup>+</sup> : 5s <sup>0</sup>	37.27 (1)
		Ag <sup>+</sup> : 4d <sup>10</sup>	$\pi_{C=N}^*$	1.560 (1)
	Py2	N: sp <sup>2</sup> lone pair	Ag <sup>+</sup> : 5s <sup>0</sup>	63.86 (2)
		Ag <sup>+</sup> : 4d <sup>10</sup>	$\pi_{C=N}^*$	2.190 (2)
	Py3	N: sp <sup>2</sup> lone pair	Ag <sup>+</sup> : 5s <sup>0</sup>	50.34 (2)
				13.24 (1)
		Ag <sup>+</sup> : 4d <sup>10</sup>	$\pi_{C=N}^*$	1.580 (2)
	Py4	N: sp <sup>2</sup> lone pair	Ag <sup>+</sup> : 5s <sup>0</sup>	26.48 (4)
[Ag(NCH) <sub>n</sub> ] <sup>+</sup>	CN1	N: sp lone pair	Ag <sup>+</sup> : 5s <sup>0</sup>	22.87 (1)
		Ag <sup>+</sup> : 4d <sup>10</sup>	$\pi_{C=N}^*$	2.340 (2)
	CN2	N: sp lone pair	Ag <sup>+</sup> : 5s <sup>0</sup>	55.69 (1)
		Ag <sup>+</sup> : 4d <sup>10</sup>	$\pi_{C=N}^*$	3.460 (4)
	CN3	N: sp lone pair	Ag <sup>+</sup> : 5s <sup>0</sup>	36.45 (3)
		Ag <sup>+</sup> : 4d <sup>10</sup>	$\pi_{C=N}^*$	1.860 (6)
	CN4	N: sp lone pair	Ag <sup>+</sup> : 5s <sup>0</sup>	34.24 (4)
		Ag <sup>+</sup> : 4d <sup>10</sup>	$\pi_{C=N}^*$	1.018 (8)

<sup>a</sup>Values in the parentheses are the number of donor–acceptor interactions. Only the interaction value above 1.00 kcal mol<sup>−1</sup> is listed.

from the aromatic ring also donate electrons to the Ag 5s orbital via the N sp<sup>2</sup> orbital.

The  $\pi$ -back donations from silver (4d)<sup>10</sup> to  $\pi_{C=N}^*$  in the case of HCN, NH=CH<sub>2</sub>, and C<sub>5</sub>H<sub>5</sub>N ligands are quite small in our study. This phenomenon was reported by Tian et al.,<sup>6</sup> where a comparison when pyridine forms complexes with different transition metals and metal ions, namely, Cu, Ag, Au, Cu<sup>+</sup>, Ag<sup>+</sup>, Au<sup>+</sup>, and Pt, is made. Since it is insignificant compared to the  $\sigma$ -donation, it thus does not need to be discussed in more detail here.

**3.4. Natural Energy Decomposition Analysis.** NEDA is a useful method for analyzing the relative importance of different interaction components constituting the overall metal ion–ligand interaction. These analyses provide additional examination of the nature of Ag<sup>+</sup>–ligand interactions in these complexes. Table 6 lists the total interaction energies per ligand along with its separated components, namely, CT for charge transfer, ES for electrostatic, POL for polarization, and XC for exchange–correlation energies. Analyzing interaction energies per ligand allows comparison within a given type of ligand but with different coordination numbers and also across different ligands. Figure 2 displays these energy components for different ligands.

The total energies per ligand of the one- and two-coordinated complexes are more negative than those of three- and four-coordinated complexes, shown in Table 6 and Figure 2. In particular, in all cases, electrostatic (ES) and charge transfer (CT) energies are dominant compared to

**Table 6. NEDA of Component Energies per Ligand (All in kcal/mol) between the Silver Ion and Ligands: Ammonia, Azomethine, Pyridine, and Hydrogen Cyanide<sup>a</sup>**

ligand	CT	ES	POL	XC	$E_{\text{total}}$
N1	-47.12	-58.79	-33.12	-20.71	-47.66
N2	-66.22	-63.52	-29.06	-22.18	-46.74
N3	-45.54	-45.02	-19.62	-16.06	-35.40
N4	-40.40	-37.16	-14.74	-13.61	-29.26
AM1	-42.62	-59.00	-48.82	-22.65	-48.95
AM2	-62.11	-64.57	-50.20	-25.98	-47.72
AM3	-40.78	-46.64	-31.68	-18.45	-35.88
AM4	-35.16	-38.12	-22.43	-14.96	-29.64
Py1	-41.94	-60.52	-65.34	-24.94	-54.19
Py2	-57.00	-64.11	-58.77	-26.77	-50.82
Py3	-36.10	-46.47	-39.25	-19.67	-37.93
Py4	-28.48	-37.60	-28.39	-15.92	-31.03
CN1	-31.72	-47.84	-52.88	-21.58	-38.16
CN2	-57.14	-54.10	-57.42	-25.37	-38.25
CN3	-39.51	-39.78	-36.30	-17.98	-29.97
CN4	-34.62	-32.33	-24.92	-14.01	-25.22

<sup>a</sup>CT: charge transfer, ES: electrostatic, XC: exchange correlation, and  $E_{\text{total}}$ : total energy.

others. The large ES energy in pyridine complexes was evaluated in the Dopfer experiment.<sup>43</sup> For all ligand types, ES energies are found to be smallest in the largest four-coordinated complex forms as expected. What is unexpected is that both ES and CT energies are found to be largest and of nearly equal magnitude in the two-coordinated form as compared to those in other coordinated forms. In each ligand type, the ES value of the two-coordinated complex is even larger than that of the one-coordinated complex where one would expect to have the largest ES interaction energy. These results suggest that the two-coordinated form with linear N–Ag<sup>+</sup>–N configuration enhances both dative bonding and electrostatic interaction in metal ion–ligand interaction, and thus, the use of the one-coordinate complex form to study bonding in transition metal complexes may not be accurate for the silver ion. The results also show that for unsaturated ligands such as azomethine, pyridine, and hydrogen cyanide, electrons in the  $\pi$  orbitals lead to reasonably large polarization interaction energy between the metal ion and the ligands. In fact, in each coordinated form, polarization energy decreases with the number of the  $\pi$ -orbital in the ligand, namely, decreases from pyridine ( $3\pi$ -orbitals) and hydrogen cyanide ( $2\pi$ -orbitals) to azomethine ( $1\pi$ -orbital).

**3.5. Effects of Nitrogen Hybrid Orbitals on Metal Complex Properties.** With respect to the effects of different nitrogen hybrid orbitals  $sp$ ,  $sp^2$ , and  $sp^3$  on properties of the Ag<sup>+</sup> complexes, we found that the bond distance decreases from  $sp^3$  to  $sp$  in each coordination number. This can be explained by the less p-character in the hybrid orbital which would lead to larger overlap with the  $5s^0$  orbital and thus shorten the bond distance. It is often known that shorter bond length corresponds to a stronger bond energy and larger vibrational frequency. However, in this case, we found that the silver ion complex with ammonia (N- $sp^3$ ) has not only the longest bond distance but also has the strongest bond energy and corresponding stretching frequency as compared to complexes with other N hybrid orbitals. This is perhaps due to binding between the Ag<sup>+</sup> ion and  $sp^2$ , and the  $sp$  N species also has  $\pi$ -back bonding from d-orbitals of the silver ion to  $\pi^*$

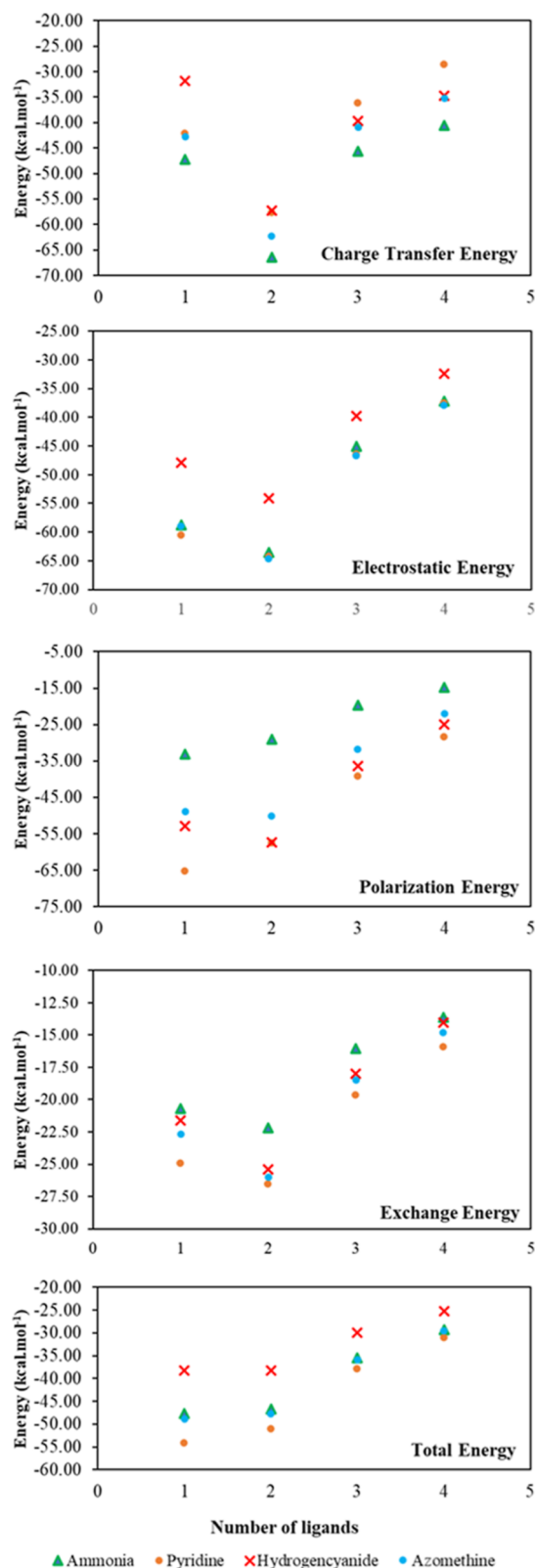


**Figure 2.** Plot of NEDA energy components: charge transfer, electrostatic, polarization, exchange correlation, and total energies of silver ion–ligand interaction. Green triangles are for silver–ammonia, blue dots for silver–azomethine, orange dots for silver–pyridine, and red crosses for silver–hydrogen cyanide complexes.

orbitals of N  $sp$  and  $sp^2$  nitrogen ligands such as with azomethine, pyridine, or hydrogen cyanide. Donating electrons

to an antibonding orbital would weaken the bonding interaction and thus lower the vibrational frequency.

#### 4. CONCLUSIONS

In this study, the nature of bonding in transition metal complexes between the silver ion  $\text{Ag}^+$  and the lone pair of nitrogen atoms in different atomic orbital hybridizations is systematically examined at the B97-1 level of DFT with a composite basis set (cc-pVTZ-pp for silver and cc-pVTZ for the other atoms). Ammonia is used to model nitrogen  $\text{sp}^3$ , azomethine and pyridine are used for  $\text{sp}^2$ , and hydrogen cyanide is used for  $\text{sp}$  hybridization. The experimental and theoretical thermodynamic data show that the one- and two-coordinated complexes of the silver ion with different types of ligands are more favorable than three- and four-coordinated silver ion complexes. Moreover, within each ligand type, the results indicate that the two-coordinated silver ion complexes are the most stable form, which have the shortest  $\text{Ag}^+-\text{N}$  bond distance, highest vibrational frequencies, and largest bond order. NEDA and natural population analyses further supporting the finding show that the two-coordinated complexes have large electrostatic and charge transfer energies per ligand basis. The results suggest that the two-coordinated complexes would be a better representation for studying bonding in silver ion–ligand interaction rather than one-coordinated complexes often used in the past.

With respect to the nature of the dative bond in these complexes, upon comparing across different nitrogen hybridizations, it is seen that the nitrogen lone pair in the  $\text{N}-\text{sp}^3$  orbital has the largest  $\sigma$ -donation to the empty silver  $5s^0$  orbital. The  $\pi$ -back donation from silver ion 4d lone pairs to  $\pi^*$  orbitals of ligands is quite small in all cases. It is found that the higher number of  $\pi$ -orbitals increases much more the polarization energy values in azomethine, hydrogen cyanide, and pyridine.

#### AUTHOR INFORMATION

##### Corresponding Author

Thanh N. Truong – Department of Chemistry, University of Utah, Salt Lake City, Utah 84112, United States;

orcid.org/0000-0003-1832-1526;

Email: Thanh.Truong@utah.edu

##### Authors

Lam H. Nguyen – Institute for Computational Science and Technology, Ho Chi Minh City 700000, Vietnam; Faculty of Chemistry, University of Science, Ho Chi Minh City 700000, Vietnam; Vietnam National University, Ho Chi Minh City 700000, Vietnam; orcid.org/0000-0003-3347-4379

Dung P. Tran – Faculty of Chemistry, Ho Chi Minh City University of Education, Ho Chi Minh City 7000000, Vietnam

Complete contact information is available at:

<https://pubs.acs.org/10.1021/acsomega.2c05707>

##### Author Contributions

All calculations are conducted and written in this manuscript. Both authors read and approved the final manuscript.

##### Funding

This work is supported in part by funding from The Office of Science and Technology, Ho Chi Minh City, Vietnam, via Institute for Computational Science and Technology in Ho

Chi Minh City with contract number 42/2020/HD-QPTKHCN.

##### Notes

The authors declare no competing financial interest.

#### ACKNOWLEDGMENTS

Authors thank the University of Utah Center and Institute for Computational Science and Technology for High-Performance Computing for computing resources.

#### ABBREVIATIONS

WBI, wiberg bond index; NEDA, natural energy decomposition analysis; NBO, natural bond orbital; NRT, natural resonance theory; BSSE, basis set superposition error

#### REFERENCES

- (1) Fox, B. S.; Beyer, M. K.; Bondybey, V. E. Coordination chemistry of silver cations. *J. Am. Chem. Soc.* **2002**, *124*, 13613–13623.
- (2) Fukino, T.; Joo, H.; Hisada, Y.; Obana, M.; Yamagishi, H.; Hikima, T.; Takata, M.; Fujita, N.; Aida, T. Manipulation of discrete nanostructures by selective modulation of noncovalent forces. *Science* **2014**, *344*, 499–504.
- (3) El-Sayed, D. S.; El-Faham, A.; Soliman, S. M. Synthesis, molecular and supramolecular structure aspects and biological evaluations of a novel  $[\text{Ag}_2(\text{phthalazine})(\text{NO}_3)_2] \cdot n \cdot 3\text{D}$  coordination polymer. *J. Mol. Struct.* **2022**, *1257*, 132592.
- (4) Potwana, F. S.; Pillay, M. N.; Staples, R. J.; Adeniyi, A. A.; Singh, P.; van Zyl, W. E. Silver (I) bis (phosphanyl amino) naphthalene complexes: Synthesis, structures and density functional theory (DFT) calculations. *Inorg. Chim. Acta* **2021**, *515*, 120041.
- (5) Shoeib, T.; Milburn, R. K.; Koyanagi, G. K.; Lavrov, V. V.; Bohme, D. K.; Siu, K. W. M.; Hopkinson, A. C. A study of complexes  $\text{Mg}(\text{NH}_3)_n$  and  $\text{Ag}(\text{NH}_3)_n$ , where  $n = 1-8$ : competition between direct coordination and solvation through hydrogen bonding. *Int. J. Mass Spectrom.* **2000**, *201*, 87–100.
- (6) Wu, D.-Y.; Ren, B.; Jiang, Y.-X.; Xu, X.; Tian, Z.-Q. Density functional study and normal-mode analysis of the bindings and vibrational frequency shifts of the pyridine–M (M = Cu, Ag, Au, Cu+, Ag+, Au+, and Pt) complexes. *J. Phys. Chem. A* **2002**, *106*, 9042–9052.
- (7) Yang, Y.-S.; Hsu, W.-Y.; Lee, H.-F.; Huang, Y.-C.; Yeh, C.-S.; Hu, C.-H. Experimental and Theoretical Studies of Metal Cation–Pyridine Complexes Containing Cu and Ag. *J. Phys. Chem. A* **1999**, *103*, 11287–11292.
- (8) Shoeib, T.; El Aribi, H.; Siu, K. M.; Hopkinson, A. C. A study of silver (I) ion–organonitrile complexes: ion structures, binding energies, and substituent effects. *J. Phys. Chem. A* **2001**, *105*, 710–719.
- (9) Luna, A.; Amekraz, B.; Tortajada, J. A theoretical study on the complexation of  $\text{sp}$ ,  $\text{sp}^2$  and  $\text{sp}^3$  nitrogen-containing species by  $\text{Cu}^+$ . *Chem. Phys. Lett.* **1997**, *266*, 31–37.
- (10) Holland, P. M.; Castleman, A., Jr The thermochemical properties of gas-phase transition metal ion complexes. *J. Chem. Phys.* **1982**, *76*, 4195–4205.
- (11) Bedin, M.; Karim, A.; Reitti, M.; Carlsson, A.-C. C.; Topić, F.; Cetina, M.; Pan, F.; Havel, V.; Al-Ameri, F.; Sindelar, V.; Rissanen, K.; Gräfenstein, J.; Erdélyi, M. Counterion influence on the  $\text{N}-\text{I}-\text{N}$  halogen bond. *Chem. Sci.* **2015**, *6*, 3746–3756.
- (12) Rodgers, M.; Stanley, J.; Amunugama, R. Periodic trends in the binding of metal ions to pyridine studied by threshold collision-induced dissociation and density functional theory. *J. Am. Chem. Soc.* **2000**, *122*, 10969–10978.
- (13) Del Piero, S.; Fedele, R.; Melchior, A.; Portanova, R.; Tolazzi, M.; Zangrando, E. Solvation effects on the stability of silver (I) complexes with pyridine-containing ligands studied by thermodynamic and DFT methods. *Inorg. Chem.* **2007**, *46*, 4683–4691.

- (14) Jones, P. G.; Roesky, H. W.; Schimkowiak, J. How do silver (I) cations react with hydrogen cyanide? The crystal structure of [Ag(NCH)<sub>2</sub>][SbF<sub>6</sub>]. *J. Chem. Soc., Chem. Commun.* **1988**, *11*, 730.
- (15) Ma, N. L. How strong is the Ag<sup>+</sup>-ligand bond? *Chem. Phys. Lett.* **1998**, *297*, 230–238.
- (16) Lo, R.; Manna, D.; Lamanec, M.; Dračinský, M.; Bouř, P.; Wu, T.; Bastien, G.; Kaleta, J.; Miriyala, V. M.; Špirko, V.; Mašínová, A.; Nachtigallová, D.; Hobza, P. The stability of covalent dative bond significantly increases with increasing solvent polarity. *Nat. Commun.* **2022**, *13*, 2107.
- (17) Jerabek, P.; Schwerdtfeger, P.; Frenking, G. Dative and electron-sharing bonding in transition metal compounds. *J. Comput. Chem.* **2019**, *40*, 247–264.
- (18) Frisch, M. J.; Trucks, G. W.; Schlegel, H. B.; Scuseria, G. E.; Robb, M. A.; Cheeseman, J. R.; Scalmani, G.; Barone, V.; Petersson, G. A.; Nakatsuji, H.; Li, X.; Caricato, M.; Marenich, A. V.; Bloino, J.; Janesko, B. G.; Gomperts, R.; Mennucci, B.; Hratchian, H. P.; Ortiz, J. V.; Izmaylov, A. F.; Sonnenberg, J. L.; Ding, F.; Lipparini, F.; Egidi, F.; Goings, J.; Peng, B.; Petrone, A.; Henderson, T.; Ranasinghe, D.; Zakrzewski, V. G.; Gao, J.; Rega, N.; Zheng, G.; Liang, W.; Hada, M.; Ehara, M.; Toyota, K.; Fukuda, R.; Hasegawa, J.; Ishida, M.; Nakajima, T.; Honda, Y.; Kitao, O.; Nakai, H.; Vreven, T.; Throssell, K.; Montgomery, J. A., Jr.; Peralta, J. E.; Ogliaro, F.; Bearpark, M. J.; Heyd, J. J.; Brothers, E. N.; Kudin, K. N.; Staroverov, V. N.; Keith, T. A.; Kobayashi, R.; Normand, J.; Raghavachari, K.; Rendell, A. P.; Burant, J. C.; Iyengar, S. S.; Tomasi, J.; Cossi, M.; Millam, J. M.; Klene, M.; Adamo, C.; Cammi, R.; Ochterski, J. W.; Martin, R. L.; Morokuma, K.; Farkas, O.; Foresman, J. B.; Fox, D. J. *Gaussian 16*; Rev. C.01: Wallingford, CT, 2016.
- (19) Hamprecht, F. A.; Cohen, A. J.; Tozer, D. J.; Handy, N. C. Development and assessment of new exchange-correlation functionals. *J. Chem. Phys.* **1998**, *109*, 6264–6271.
- (20) Li, S.; Peterson, K. A.; Dixon, D. A. Benchmark calculations on the adiabatic ionization potentials of M–NH<sub>3</sub> (M = Na, Al, Ga, In, Cu, Ag). *J. Chem. Phys.* **2008**, *128*, 154301.
- (21) Malik, M.; Wysokiński, R.; Zierkiewicz, W.; Helios, K.; Michalska, D. Raman and infrared spectroscopy, DFT calculations, and vibrational assignment of the anticancer agent picoplatin: performance of long-range corrected/hybrid functionals for a platinum (II) complex. *J. Phys. Chem. A* **2014**, *118*, 6922–6934.
- (22) Cramer, C. J.; Truhlar, D. G. Density functional theory for transition metals and transition metal chemistry. *Phys. Chem. Chem. Phys.* **2009**, *11*, 10757–10816.
- (23) Schultz, N. E.; Gherman, B. F.; Cramer, C. J.; Truhlar, D. G. Pd n CO (n = 1, 2): Accurate ab initio bond energies, geometries, and dipole moments and the applicability of density functional theory for fuel cell modeling. *J. Phys. Chem. B* **2006**, *110*, 24030–24046.
- (24) Woon, D. E.; Dunning, T. H., Jr. Gaussian basis sets for use in correlated molecular calculations. IV. Calculation of static electrical response properties. *J. Chem. Phys.* **1994**, *100*, 2975–2988.
- (25) Sherrill, C. D. *Counterpoise Correction and Basis Set Superposition Error*; School of Chemistry and Biochemistry Georgia Institute of Technology, 2010.
- (26) Truhlar, D. G. A simple approximation for the vibrational partition function of a hindered internal rotation. *J. Comput. Chem.* **1991**, *12*, 266–270.
- (27) Glendening, E. D.; Streitwieser, A. Natural energy decomposition analysis: An energy partitioning procedure for molecular interactions with application to weak hydrogen bonding, strong ionic, and moderate donor–acceptor interactions. *J. Chem. Phys.* **1994**, *100*, 2900–2909.
- (28) Weinhold, F. *Discovering Chemistry with Natural Bond Orbitals*; John Wiley & Sons, 2012.
- (29) Mitoraj, M. P.; Michalak, A.; Ziegler, T. A combined charge and energy decomposition scheme for bond analysis. *J. Chem. Theory Comput.* **2009**, *5*, 962–975.
- (30) Li, T.-L.; Lu, W.-C. Energy decomposition analysis of cationic carbene analogues with group 13 and 16 elements as a central atom: a comparative study. *Phys. Chem. Chem. Phys.* **2022**, *24*, 8970–8978.
- (31) Glendening, E. D. Natural energy decomposition analysis: Extension to density functional methods and analysis of cooperative effects in water clusters. *J. Phys. Chem. A* **2005**, *109*, 11936–11940.
- (32) Smith, B. A.; Vogiatzis, K. D.  $\sigma$ -Donation and  $\pi$ -Backdonation Effects in Dative Bonds of Main-Group Elements. *J. Phys. Chem. A* **2021**, *125*, 7956–7966.
- (33) Khireche, M.; Zouchoune, B.; Ferhati, A.; Nemdili, H.; Zerizer, M. A. Understanding the chemical bonding in sandwich complexes of transition metals coordinated to nine-membered rings: energy decomposition analysis and the donor–acceptor charge transfers. *Theor. Chem. Acc.* **2021**, *140*, 122.
- (34) Bowmaker, G. A.; Effendy, K. C.; Lim, B. W.; Skelton, D.; Sukarianingsih, A. H.; White, A. H. Syntheses, structures and vibrational spectroscopy of some 1: 2 and 1: 3 adducts of silver (I) oxanion salts with pyridine and piperidine bases containing non-coordinating 2, (6)-substituents. *Inorg. Chim. Acta* **2005**, *358*, 4342–4370.
- (35) Miles, M.; Patterson, J.; Hobbs, C.; Hopper, M.; Overend, J.; Tobias, R. Raman and infrared spectra of isosteric diammine and dimethyl complexes of heavy metals. Normal-coordinate analysis of (X<sub>3</sub>Y<sub>2</sub>)<sub>2</sub>Z ions and molecules. *Inorg. Chem.* **1968**, *7*, 1721–1729.
- (36) Geddes, A. L.; Bottger, G. L. Infrared spectra of silver-ammine complexes. *Inorg. Chem.* **1969**, *8*, 802–807.
- (37) Nilsson, K. B.; Persson, I.; Kessler, V. G. Coordination chemistry of the solvated AgI and AuI ions in liquid and aqueous ammonia, trialkyl and triphenyl phosphite, and tri-*n*-butylphosphine solutions. *Inorg. Chem.* **2006**, *45*, 6912–6921.
- (38) Nockemann, P.; Meyer, G. [Ag(NH<sub>3</sub>)<sub>2</sub>]ClO<sub>4</sub>: Kristallstrukturen, Phasenumwandlung, Schwingungsspektren. *Z. Anorg. Allg. Chem.* **2002**, *628*, 1636–1640.
- (39) Dyason, J.; Healy, P.; Engelhardt, L.; White, A. Lewis-Base Adducts of Group 1B Metal (I) Compounds. XXII. Crystal Structure of Bis (pyridine) silver (I) Perchlorate. *Aust. J. Chem.* **1985**, *38*, 1325–1328.
- (40) Rogovoy, M. I.; Frolova, T. S.; Samsonenko, D. G.; Berezin, A. S.; Bagryanskaya, I. Y.; Nedolya, N. A.; Tarasova, O. A.; Fedin, V. P.; Artem'ev, A. V. 0D to 3D coordination assemblies engineered on 2-(alkylsulfanyl) azine ligands: crystal structures, dual luminescence and cytotoxic activity. *Eur. J. Inorg. Chem.* **2020**, *2020*, 1635–1644.
- (41) Behera, P. K.; Kisan, H. K.; Isab, A. A.; Dinda, J. Novel synthesis, structural characterization, DFT and TDDFT investigation of 'Butterfly'like Ag (I)-complex supported by 3-pyrazinyl [1-methyl] imidazolium hexafluorophosphate. *J. Mol. Struct.* **2021**, *1235*, 130188.
- (42) Weinhold, F.; Landis, C. R. Natural bond orbitals and extensions of localized bonding concepts. *Chem. Educ. Res. Pract.* **2001**, *2*, 91–104.
- (43) Chakraborty, S.; Dopfer, O. Infrared Spectrum of the Ag<sup>+</sup>–(Pyridine)<sub>2</sub> Ionic Complex: Probing Interactions in Artificial Metal-Mediated Base Pairing. *ChemPhysChem* **2011**, *12*, 1999–2008.